Myrtucommulone from *Myrtus communis*: Metabolism, Permeability, and Systemic Exposure in Rats

Authors

Kathleen Gerbeth[1], Jan Hüsch[1], Jürgen Meins[1], Antonietta Rossi[2], Lidia Sautebin[2], Katja Wiechmann[3], Oliver Werz[3], Carsten Skarke[4], Jeffrey S. Barrett[5], Manfred Schubert-Zsilavecz[1,6], Mona Abdel-Tawab[1]

Affiliations

The affiliations are listed at the end of the article

Abstract

▼

Nonsteroidal anti-inflammatory drug intake is associated with a high prevalence of gastrointestinal side effects, and severe cardiovascular adverse reactions challenged the initial enthusiasm in cyclooxygenase-2 inhibitors. Recently, it was shown that myrtucommulone, the active ingredient of the Mediterranean shrub *Myrtus communis*, dually and potently inhibits microsomal prostaglandin E_2 synthase-1 and 5-lipoxygenase, suggesting a substantial anti-inflammatory potential. However, one of the most important prerequisites for the anti-inflammatory effects *in vivo* is sufficient bioavailability of myrtucommulone. Therefore, the present study was aimed to determine the permeability and metabolic stability *in vitro* as well as the systemic exposure of myrtucommulone in rats. Permeation studies in the Caco-2 model revealed apparent permeability coefficient values of $35.9 \cdot 10^{-6}$ cm/s at 37 °C in the apical to basolateral direction, indicating a high absorption of myrtucommulone. In a pilot rat study, average plasma levels of 258.67 ng/mL were reached 1 h after oral administration of 4 mg/kg myrtucommulone. We found that myrtucommulone undergoes extensive phase I metabolism in human and rat liver microsomes, yielding hydroxylated and bihydroxylated as well as demethylated metabolites. Physiologically-based pharmacokinetic modeling of myrtucommulone in the rat revealed rapid and extensive distribution of myrtucommu-lone in target tissues including plasma, skin, muscle, and brain. As the development of selective microsomal prostaglandin E_2 synthase-1 inhibitors represents an interesting alternative strategy to traditional nonsteroidal anti-inflammatory drugs and cyclooxygenase-2 inhibitors for the treatment of chronic inflammation, the present study encourages further detailed pharmacokinetic investigations on myrtucommulone.

Abbreviations

▼

COXIBs:	cyclooxygenase-2 inhibitors
HBSS:	Hanks buffered salt solution
HLM:	human liver microsomes
LC:	liquid chromatography
5-LO:	5-lipoxygenase
mPGES:	microsomal prostaglandin E_2 synthase
MC:	myrtucommulone
MRM:	multiple-reaction monitoring
NSAIDs:	nonsteroidal anti-inflammatory drugs
P_{app}:	apparent permeability coefficient
PBPK:	physiologically-based pharmacokinetic modeling
Pgp:	P-glycoprotein
RLM:	rat liver microsomes
TEER:	transepithelial electrical resistance
UGT:	uridine glucuronosyltransferase
DMEM:	Dulbecco's modified Eagle's medium

Introduction

▼

Being far from a real breakthrough in the discovery of safe NSAIDs [1], interest in alternative well-tolerated anti-inflammatory herbal remedies is growing.

Myrtle (*Myrtus communis,* Myrtaceae) is a Mediterranean shrub applied as a culinary spice and flavoring agent for alcoholic beverages [2,3]. In traditional folk medicine it has been used as an antiseptic, antidiabetic, and anti-inflammatory remedy. Scientific studies support the antibacterial [4], antihyperglycemic [5,6], analgesic [7], and antioxidant [8–10] properties. Recently, antiproliferative, antibacterial, and anti-inflammatory effects of the ethanolic myrtle extract Myrta-

cine® in keratinocytes were reported, suggesting a therapeutic value in the treatment of acne [11]. It was shown that MC (○ Fig. 1) suppresses the biosynthesis of eicosanoids by direct inhibition of key enzymes like COX-1 and 5-LO in cell-free and cell-based models [3]. Moreover, MC inhibits the mPGES-1-mediated conversion of PGH_2 to PGE_2 in cell-free assays [12] as well as in intact A549 cells and in human whole blood [12]. *In vivo*, i. p. administration of MC (0.5, 1.5, and 4.5 mg/kg) reduced the development of mouse carrageenan-induced paw edema in a dose-dependent manner and exerted anti-inflammatory efficacy in the pleurisy model in mice [13]. However, no bioavailability studies have been performed yet in animals or humans. Since poor absorption and/or extensive metabolism may play a crucial role in limiting systemic availability, the present study aimed to determine the permeability of MC in Caco-2 cells and its metabolic stability in rat and human liver microsomes as well as its oral availability in a pilot rat study. Moreover, PBPK was applied to estimate the distribution of MC in potential target tissues.

Fig. 1 Chemical structures of **a** MC and **b** hyperforin.

Material and Methods
▼
Standards and reagents
MC with a purity of 99% was synthesized by Prof. Johann Jauch, University of Saarland, Dept. of Organic Chemistry, Saarbruecken, Germany [14]. Hyperforin dicyclohexyl ammonium salt (purity 99%), used as an internal standard, was supplied by Dr. W. Schwabe Arzneimittel GmbH. Other reagents included tetrahydrofurane (gradient grade; Acros Organics SA), acetonitrile for LC-MS (Sigma-Aldrich), distilled water, *tert*-butyl methyl ether, ethyl acetate (Merck), and ammonium formate (p. a.; VWR). Blank human plasma was obtained from Deutsches Rotes Kreuz-Blutspendedienst, Mannheim, Germany. Pooled HLM, RLM, NADPH-regenerating solutions A and B, and UGT reaction mix solutions were purchased from BD Biosciences.

Caco-2 cells were seeded on Transwell® polycarbonate inserts with a mean pore size of 0.4 µm (Corning Incorporated) and were grown in DMEM, containing 25 mM glucose supplemented with 10% FCS, 1% nonessential amino acids, and gentamycine (0.1 mg/mL). All media and HBSS were purchased from Biochrom AG. HEPES, FITC-dextran, propranolol hydrochloride, and verapamil were received from Sigma-Aldrich.

Microsomal incubation and sample preparation
MC stock solution (250 µg/mL) was prepared in acetonitrile-water (50 : 50, v/v). The final incubation solutions for phase I reactions contained 50 mM potassium phosphate buffer (pH 7.4), 7.5 µM MC, 1.3 µM NADP+, 3.3 mM glucose-6-phosphate, 3.3 mM $MgCl_2$, and 0.4 U/mL glucose-6-phosphate dehydrogenase in a total volume of 250 µL. For phase II reactions, the final incubation solutions consisted of 162.5 µL water, 20 µL of the UGT reaction mix solution A containing 2 mM UDP-glucuronic acid cofactor, 50 µL of the UGT reaction mix solution B (50 mM Tris-HCl, 8 mM $MgCl_2$, 25 µg/mL alamethicin), and MC (7.5 µM) in a total volume of 250 µL. Reaction was initiated by the addition of 12.5 µL liver microsomes (1 mg/mL). The concentration of 7.5 µM was chosen on the recommendation of the manufacturer. Controls were prepared without cofactors. Aliquots of 50 µL were withdrawn after 15, 30, 60, and 120 min from phase I incubations. Phase II incubation was stopped after 2 h by the addition of equal amounts of ice-cold internal standard solution in acetonitrile. The samples were kept on ice for 15 min followed by centrifugation for
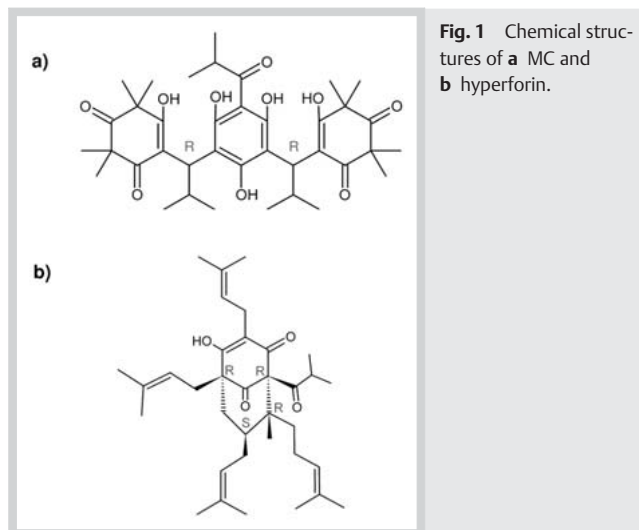
15 min (2500 g, at 4 °C). Afterwards, the supernatants were diluted 1 : 50 and analyzed directly by LC-MS/MS in the multiple reaction monitoring mode. Metabolic stability of MC was determined in triplicate at each time point and after 2 h in case of the phase II glucuronidation experiments.

Permeation of MC in the Caco-2 model
MC stock solution (1 mg/mL) was prepared in DMSO. Then, 100 µL of the stock solution were diluted with HBSS containing 20 mM HEPES adjusted to pH 6.5 (apical site) or pH 7.4 (basolateral site) to yield a final concentration of 10 µg/mL MC and 1% DMSO. This MC concentration was chosen to allow its detection at the basolateral side even in case of poor permeability. For testing the interaction of MC with P-glycoprotein (Pgp), the Pgp substrate verapamil (50 µM) was added to the working solutions. Permeation of MC was investigated in both directions at 37 °C with and without verapamil (50 µM) and additionally at 4 °C in the apical-to-basolateral (AB) direction (n = 6 each).

Prior to each experiment, Caco-2 monolayers were washed with HBSS. TEER was measured before and after the transport experiments. FITC-Dextran (MW 4400 g/mol) was used to gauge the integrity of the monolayers. Transports with propranolol hydrochloride (n = 3) served as a positive control for the functionality of every cell passage. During incubation, the plates were agitated at 37 °C on a shaker at 120 rpm. Receiver fluid was withdrawn after 15, 30, 60, 75, and 90 min and replaced by equal volumes of fresh buffer solution. At the end of the experiment, samples were collected from both sides, and the plates were washed three times with pure HBSS followed by methanol. Then, each transwell filter was cut off, placed in 0.5 mL methanol for 15 min and vortexed in order to lyse the cells. All samples were stored at −20 °C. For analysis, an aliquot of 150 µL was mixed with equal amounts of acetonitrile containing the I. S. at a concentration of 200 ng/mL. Solutions of pure methanol from cell lysis were evaporated to dryness and reconstituted in a mixture of acetonitrile/buffer containing the internal standard before injection into the LC-MS system.

Calculation of permeability coefficients
The permeability coefficient (cm/s) was calculated by the following equation:

$$P_{app} = \frac{dc}{dt} \times \frac{V_r}{AC_0}$$

where dC/dt is the flux rate ($\mu g/(mL \times s)$) through the monolayer; V_r is the volume of the receiver chamber (mL); A is the surface area of the cell monolayer; and C_0 is the initial concentration of the donor fluid ($\mu g/mL$).

Animal study

The rat study was approved by the local ethical committee on the 2nd November 2009 and given the approval number 2009/0017055. Male Wistar Han rats (250 g; Harlan) were provided with standard rodent chow and water in a controlled environment. Animal care complied with Italian regulations on protection of animals used for experimental and other scientific purposes (Ministerial Decree 116192) as well as with the European Economic Community regulations (Official Journal of E.C. L 358/1 12/18/1986).

Following an overnight fast, 4 mg/kg MC (0.5 mL of a MC-solution 2 mg/mL) were orally administered to three rats. The control group (n = 3) received vehicle (0.5 mL) consisting of 0.5% carboxymethylcellulose and 10% Tween-20. Food was allowed 4 h after MC administration. Blood samples were taken from treated rats 1, 4, 8, 14, 24, and 48 h after MC administration and from vehicle-treated rats 4 h after vehicle administration. Approximately 4 mL blood were collected by intracardiac puncture into citrate tubes (0.1 M). Blood samples were centrifuged, and the supernatants (plasma fraction) were stored at −20 °C until analysis.

Sample preparation of rat plasma samples

Based on the LC-MS/MS method described elsewhere [15] demonstrating cross-validation between rat and human plasma, calibration samples were prepared by spiking 1 mL of human plasma with 50 µL of the particular spike solution to achieve concentrations of 1.0, 2.5, 5.0, 10.0, 25.0, 50.0, 75.0, and 100.0 ng/mL of MC, respectively. Accordingly, 1 mL of thawed plasma samples was spiked with 50 µL acetonitrile. Furthermore, 50 µL of the I.S. solution containing 100 ng internal standard were added to all samples.

Following extraction for 25 min with 5 mL 20% ethyl acetate in *tert*-butyl methyl ether in a horizontal position on a flatbed mixer and centrifugation for 15 min (2500 g, 10 °C), the organic layer was evaporated to dryness, and the residue was redissolved in 100 µL mobile phase. Then, the samples were sonicated for another minute and centrifuged for 5 min (2500 g, 10 °C). Finally, 50 µL of the supernatant were injected into the LC-MS/MS system. Samples showing a concentration > 100 ng/mL were diluted 1 : 10 in order to fit the validated concentration range.

LC-MS/MS

Liquid chromatography was performed on an Agilent 1200 series with a Gemini C6 phenyl column (Phenomenex), 250 × 4.6 mm i.d.; 5 µm and a Gemini C6 phenyl security guard cartridge (Phenomenex) 4 × 3 mm at a flow rate of 0.6 mL/min and column temperature of 40 °C in a run time of 15 min. The mobile phase consisted of acetonitrile : water (85 : 15 v/v) containing 6 mM ammonium formate. The chromatographic run was divided into three time segments starting with 0–5 min running into waste, followed by 5–12 min directed towards MS and finally 12–15 min running into waste again.

MS analysis was performed on an Agilent Triple Quad mass spectrometer equipped with an ESI source in the negative ion mode at 300 °C. The precursor ion at *m/z* 667.5 and the fragment ion of highest intensity at *m/z* 195.0 were selected for MRM of MC; similarly, the ions at *m/z* 535.5 and 383.2 were used for the internal

standard hyperforin. Data acquisition and processing was carried out with the Mass Hunter software. The detailed method and its validation are published elsewhere [15]. In brief, linearity could be proven in the range of 1–100 ng/mL with r > 0.998. The greatest deviation of the calculated from the nominal concentration was found to be − 13.8% at the low concentration level. The relative standard deviation ranged between 1.4% at the high and 11.8% at the low concentration level, meeting thus the requirements for accuracy and precision for bioanalytical methods [16]. The mean relative recoveries of MC were determined to be 92.9 ± 9.1%, 76.0 ± 12.2%, and 79.5 ± 2.1% at the low, mid, and high concentration level, respectively. In plasma, MC was found to be stable upon storage at room temperature for at least 6 h and at −20 °C for at least 6 months. Processed samples of MC were stable in the autosampler for at least 24 h. Moreover, the stability of MC was not affected by three freeze/thaw cycles.

HPLC-UV

For the determination of propranolol hydrochloride, standard solutions at concentrations of 0.207, 7.4, and 37.0 µg/mL were prepared by dissolving propranolol in methanol and diluting the stock solution with transport buffer (HBSS). Chromatographic separation was achieved within 4 min using an endcapped RP-18 column (Purospher 125 mm × 4 mm, 5 µm particle size; Agilent) at a flow rate of 0.8 mL/min (isocratic conditions). The mobile phase consisted of methanol : 0.1 M sodium dihydrogenphosphate solution pH 3.0, (60 : 40, v/v). Samples were detected by a photo diode array detector (Agilent Technologies) at 230 nm. Sample concentration was calculated using the Mass Hunter software.

Pharmacokinetics and PBPK modeling

Basic pharmacokinetic parameters (peak concentrations, C_{max}; concentration peak time, t_{max}; area-under-the-curve, AUC_{0-t}; and elimination half-life, $t_{1/2}$) for MC were determined by the statistical software package BiAS (v10.0). The PKSim (version 4.1; Bayer Technology Services GmbH) algorithm was utilized for the present PBPK model in the rat [17, 18]. Based on the lipophilicity and solubility of MC blood flow, limited partitioning was assumed. Initial inputs to the model for MC included molecular weight (668.4 D), calculated LogP of 4.5 (based on structure), measured a pKa of 5, measured aqueous solubility of 90 µM, measured protein binding of 99.9% (using ultracentrifugation), and an estimated oral clearance of 4.7 L/h/kg based on the mean concentration-time data obtained in this study.

Results and Discussion
▼

MC undergoes extensive phase I metabolism in human liver microsomes. Thus after 15 min of incubation with HLM, more than 50% of the initial MC was metabolized, and around 10% remained after 120 min. In RLM, phase I metabolism also occurred at an extensive but overall slower rate with nearly 100% of the initial MC concentration being detectable after 15 min, decreasing to 70% after 30 min, ending up with 45% after 120 min incubation time. Just as the control incubations without cofactors, the glucuronidation experiments showed no decrease in MC concentration, suggesting that MC is not susceptible to glucuronidation (data not shown).

Screening of the incubation solutions in the full-scan modus revealed various metabolites with mass shifts of + 16, + 32, and
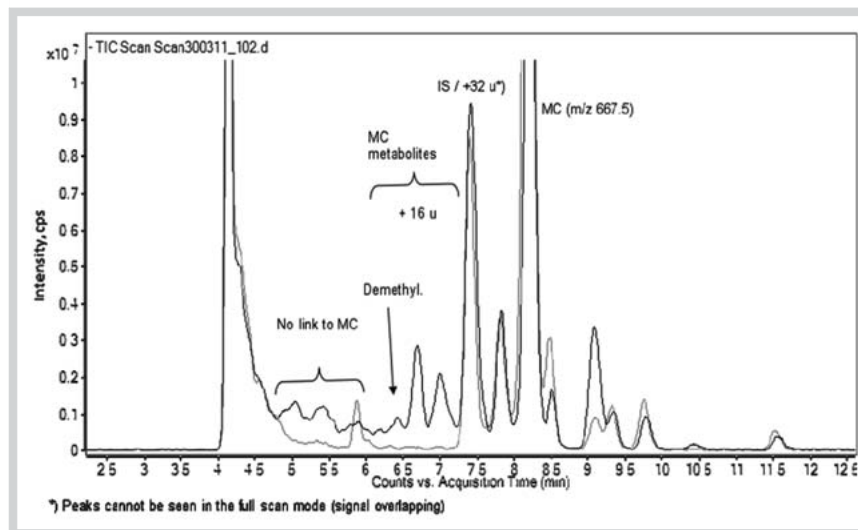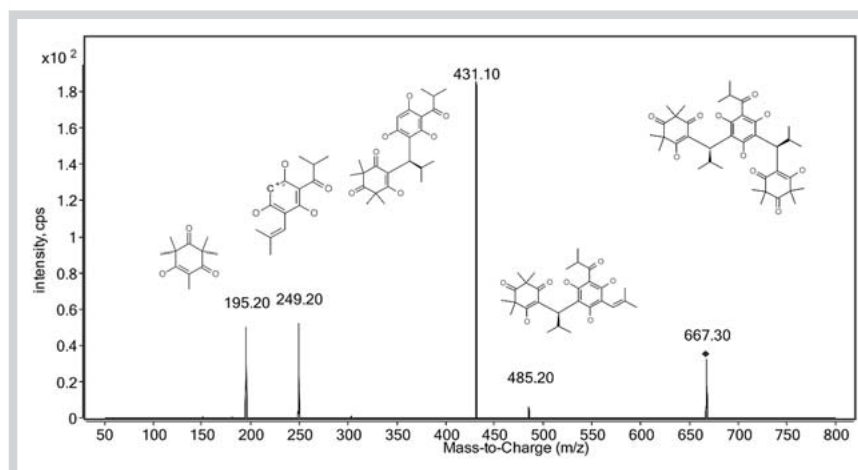
Fig. 3 Characteristic fragmentation pattern of MC.

− 14 u compared to MC that could not be detected in the control samples (○ **Fig. 2**). They were identified on the basis of their comparable fragmentation pattern with MC (○ **Fig. 3**). Product ion scans were performed to confirm the full scan results (○ **Fig. 4**). Ion masses of m/z 698.4 (MC + 2OH), 683.2 (MC + OH), 667.5 (MC), 653.4 (MC −CH$_3$), 623.4 (MC −C$_3$H$_7$) were chosen as precursor ions. Control samples revealed only the peaks at t = 4.1 min and 8.1 min (MC). Both the peak at 4.1 min and the peak at 5.6 min in the incubation solution did not yield the characteristic MC fragmentation pattern, indicating no relation to MC (peaks No. 1 and 2 in ○ **Table 1**). The other peaks showed one or more characteristic fragments of MC indicating a link to the parent compound (○ **Table 1**). Peaks No. 3 and 5 yielded the parent compound, suggesting the formation of some polar metabolites that are obviously unstable in the mass spectrometer fragmenting immediately to MC. Hence, it may be concluded that phase I metabolism results in hydroxylated, bihydroxylated, and demethylated metabolites and some other minor polar compounds. Screening of plasma samples from MC-treated rats confirmed the presence of these metabolites and the absence of glucuronidated conjugates. Moreover no sulphated conjugates could be identified in rats, suggesting that MC is mainly subject to phase I but not to phase II metabolism.

An almost linear transport of MC was observed across the Caco-2 monolayer (○ **Fig. 5**), the validity of which was proven by TEER values > 250 Ω cm^2, the impermeability of FITC-dextran, and P$_{app}$ values of propranolol (34.66·10^{-6} cm/s) corresponding to the literature [19,20]. In the AB direction, MC was highly permeable with P$_{app}$ values of 35.9·10^{-6} cm/s at 37 °C and 14.1·10^{-6} cm/s at 4 °C.
The addition of verapamil at 37 °C resulted in a P$_{app}$ value of 14.0·10^{-6} cm/s, indicating that MC is not a Pgp substrate as the MC concentrations in the receiver compartment were not increased. The lower P$_{app}$ value at 4 °C suggests that active transport (sensitive to temperature) may play a role in the absorption of MC. As expected, P$_{app}$ values were lower in the basolateral-to-apical BA direction than in the absorptive direction. At 37 °C, the BA P$_{app}$ values were determined to be 3.1·10^{-6} cm/s and 4.4·10^{-6} cm/s upon the addition of verapamil, indicating that MC is not subject to secretion processes. Around 29.8–53.9 % of the initial MC concentration was detected in the cells in the absorptive and 5.3–9.2 % in the secretory direction. However, because of the high P$_{app}$ value in the absorptive direction, accumulation in the cells and/or in the filter membrane was not paid further attention. The observed high MC permeability, in spite of its relatively high MW (667 Da) and low aqueous solubility of 90 µM, may be thus attributed to its lipophilicity and possible participa-
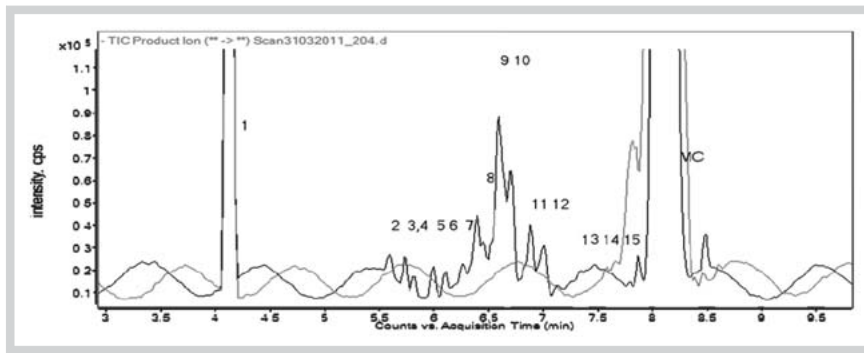
Fig. 4 Product ion scan of MC incubation solution (black line) in HLM containing NADPH-regenerating system in comparison to MC control sample (gray line) lacking cofactor solutions.

Table 1 Overview of MC metabolites (product ion scan).

| Peak number	Retention time (min)	Product ion	Characteristic fragment	Metabolism
1	4.1	483.2	–	–
2	5.6	667.5	–	–
3	5.7	667.5	431.5	unknown
4	5.8	653.4	415.4	demethylation
5	5.9	667.5	429.0	unknown
6	6.1	653.4	416.9	demethylation
7	6.25	623.4	428.6	demethylation
8	6.4	623.4	429.0	demethylation
9	6.6	683.2	446.6; 265.3	hydroxylation
10	6.7	652.1	249.2; 431.1	demethylation
11	6.9	626.2	195.1; 249.2; 431.1; 485.2	demethylation
12	7.0	625.9; 626.7	195.1; 431.1	demethylation
13	7.1	653.4	416.9	demethylation
14	7.2	698.1	195.1; 249.2; 431.1	dihydroxylation
15	7.3	697.6	431.1	dihydroxylation
MC	8.1	667.5	195.1; 249.2; 431.3; 485.2	parent compound
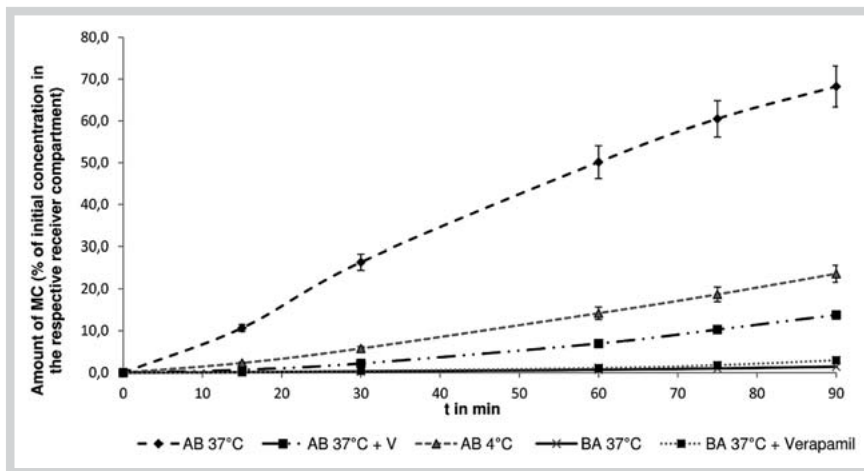
Fig. 5 Amount of MC (% of the initial concentration) transported over the time (0–90 min) under different conditions in the Caco-2 model.

tion of active transport carriers in absorption. According to Yee, P_{app} values $> 10 \cdot 10^{-6}$ cm/s reflect high absorption *in vivo* [20, 21]. Hence it may be assumed that MC, not being subject to active efflux mechanisms, might be well absorbed in humans.

After oral administration of 4 mg/kg MC to rats, maximum plasma concentrations of 190.0, 182.7, and 403.3 ng/mL were consistently attained at 1 hour post-dose. The areas under the plasma concentration curve $AUC_{0-48\,h}$ (calculated using the trapezoidal rule in SigmaPlot v11.0) were 658.3, 548.1, and 1646.9 ng/mL*h, respectively. Parameter estimates obtained from the mean con-

centration-time curve as depicted in ○ **Fig. 6** (top) are C_{max} of 258.6 ng/mL, t_{max} of 1 h, and a t½ of 10.3 h. The achieved plasma levels exceeded the expectations regarding the availability of a non-soluble, highly lipophilic, metabolically instable drug and may be attributed to the high permeability of MC observed in the Caco-2 model. Based on the applied dose and the resulting mean plasma concentration-time curve, a clearance (CL/F) of 4.7 L/h/kg, and a volume of distribution (Vd/F) of 70.1 L/kg may be assumed. The calculated clearance is in line with the extensive metabolism observed for MC *in vitro*. Furthermore, the high vol-
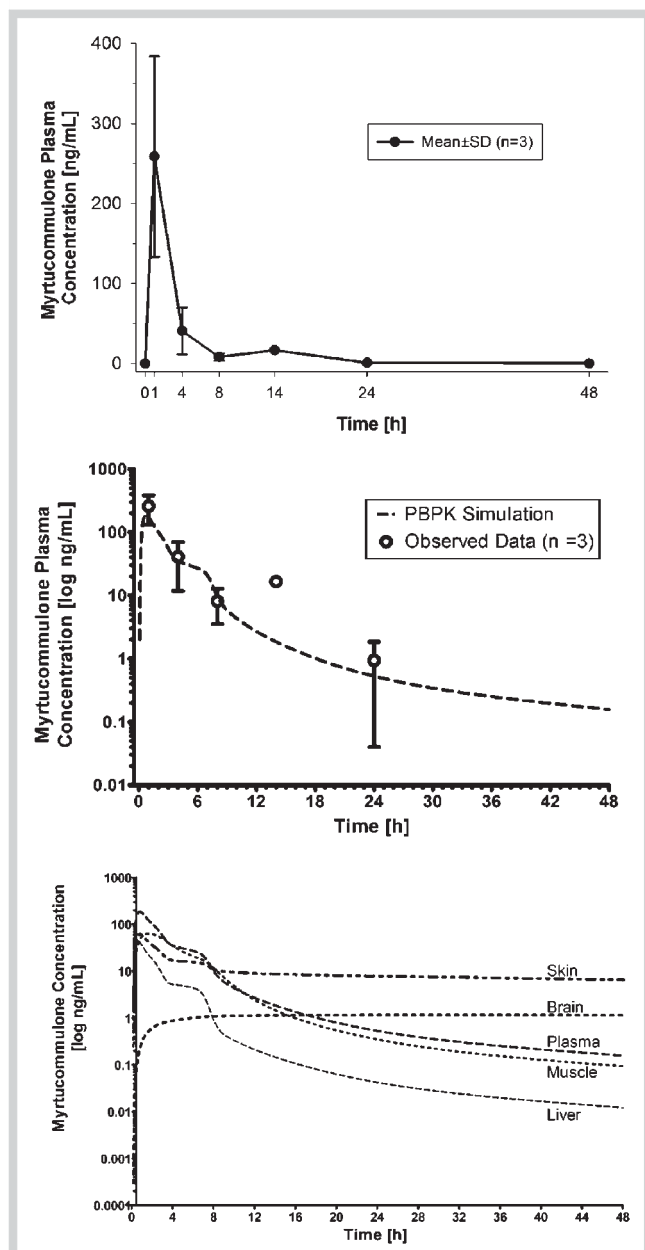
Fig. 6 Top: Average plasma concentration profile of MC after oral administration of 4 mg/kg MC to rats. The values represent the mean concentrations ± SD of three rats. The 14-h value could not be analyzed in two rats because of too small blood volume. Center: Simulated MC plasma-concentration profiles in rats in comparison to the observed plasma concentrations. Circles are mean values ± SD of three rats, with the exception of the 14-h value. Bottom: Simulated distribution of MC in different target tissues based on PBPK modeling.

ume of distribution indicates an intensive uptake of MC in various tissues. Nevertheless, given the small number of animals in this pilot study, verification of the obtained parameter estimates is recommended in studies of a larger scale. No physical signs of distress were noted in any of the three rats during the study.

Finally, PBPK modeling was applied to provide insights into the disposition of MC in potential target tissues. As seen in ⊙ Fig. 6, center, the observed and simulated plasma-concentration-time profiles of MC were comparable, indicating the suitability of the applied PBPK model to predict systemic MC exposure. According

to this model, a rapid and extensive drug distribution is suggested, which is underlined by the high volume of distribution determined for MC (⊙ Fig. 6, bottom). Notably, highly perfused tissues (e.g., liver) mimic the plasma concentration time course. Tissue exposures predicted for skin, muscle, and brain indicate that multicompartment kinetic behavior is likely and that some degree of accumulation in these organs is possible. It may be assumed that MC reaches a plateau in the skin and brain after single oral dosing that exceeds the plasma concentrations at the end of the dosing interval. This underlines the pharmacological effects of MC proposed in a keratinocyte model [11]. In contrast to skin, data on potential effects of MC on the central nervous system do not exist yet, but the observed accumulation of MC in brain tissue encourages further studies evaluating possible anti-inflammatory actions in the CNS. Of course, these simulations represent a preliminary projection of MC disposition in rats and should be confirmed by future biodistribution studies.

Against the background that selective mPGES-1 inhibitors represent an interesting alternative strategy to traditional NSAIDs and COXIBs for the treatment of chronic inflammation [22], the present study encourages further detailed pharmacokinetic investigations on MC.

Conflict of Interest
▼

The authors certify that there is no conflict of interest with any financial organization regarding the material discussed in the manuscript.

Affiliations
1 Central Laboratory of German Pharmacists, Eschborn, Germany
2 Dept. of Experimental Pharmacology, University of Naples Federico II, Naples, Italy
3 Chair of Pharmaceutical/Medicinal Chemistry, Institute of Pharmacy, University of Jena, Jena, Germany
4 Institute for Translational Medicine and Therapeutics, Dept. of Pharmacology, University of Pennsylvania Perelman School of Medicine, Philadelphia, PA, USA
5 Clinical Pharmacology & Therapeutics Division, The Children's Hospital of Philadelphia, Philadelphia, PA, USA
6 Institute of Pharmaceutical Chemistry, J. W. Goethe-University, ZAFES, Frankfurt, Germany

References
1 *Abdel-Tawab M, Zettl H, Schubert-Zsilavecz M.* Non-steroidal anti-inflammatory drugs: a critical review on current concepts applied to reduce gastrointestinal toxicity. Curr Med Chem 2009; 16: 475–481
2 *Appendino G, Bianchi F, Minassi A, Sterner O, Ballero M, Gibbons S.* Oligomeric acylphloroglucinols from myrtle (*Myrtus communis*). J Nat Prod 2002; 65: 334–338
3 *Feißt C, Franke L, Appendino G, Werz O.* Identification of molecular targets of the oligomeric nonprenylated acylphloroglucinols from *Myrtus communis* and their implication as anti-inflammatory compounds. J Pharm Exp Ther 2005; 315: 389–396
4 *Bonjar GH.* Antibacterial screening of plants used in Iranian folkloric medicine. Fitoterapia 2004; 75: 231–235
5 *Elfellah MS, Akhter MH, Khan MT.* Anti-hyperglycaemic effect of an extract of *Myrtus communis* in streptozotocin-induced diabetes in mice. J Ethnopharmacol 1984; 11: 275–281
6 *Sepici A, Gürbüz I, Cevik C, Yesilada E.* Hypoglycaemic effects of myrtle oil in normal and alloxan-diabetic rabbits. J Ethnopharmacol 2004; 93: 311–318
7 *Levesque H, Lafont O.* Aspirin throughout the ages: a historical review. Rev Med Interne 2000; 21 (Suppl. 1): 8 s–17 s
8 *Hayder N, Abdelwahed A, Kilani S, Ammar RB, Mahmoud A, Ghedira K, Chekir-Ghedira L.* Anti-genotoxic and free-radical scavenging activities of extracts from (Tunisian) *Myrtus communis*. Mutat Res 2004; 564: 89–95

9 *Romani A, Coinu R, Carta S, Pinelli P, Galvardi C, Vincieri FF, Franconi F.* Evaluation of antioxidant effect of different extracts of *Myrtus communis* L. Free Radic Res 2004; 38: 97–103

10 *Rosa A, Deiana M, Casu V, Corona G, Appendino G, Bianchi F, Ballero M, Dessi MA.* Antioxidant activity of oligomeric acylphloroglucinols from *Myrtus communis* L. Free Radic Res 2003; 37: 1013–1019

11 *Fiorini-Puybaret C, Aries MF, Fabre B, Mamatas S, Luc J, Degouy A, Ambonati M, Mejean C, Poli F.* Pharmacological properties of Myrtacine® and its potential value in acne treatment. Planta Med 2011; 77: 1582–1589

12 *Koeberle A, Pollastro F, Northoff H, Werz O.* Myrtucommulone, a natural acylphloroglucinol, inhibits microsomal prostaglandin E(2) synthase-1. Br J Pharmacol 2009; 156: 952–961

13 *Rossi A, Paola RD, Mazzon E, Genovese T, Caminiti R, Bramanti P, Pergola C, Koeberle A, Werz O, Sautebin L, Cuzzocrea S.* Myrtucommulone from *Myrtus communis* exhibits potent anti-inflammatory effectiveness *in vivo*. J Pharm Exp Ther 2009; 329: 76–86

14 *Müller H, Paul M, Hartmann D, Huch V, Blaesius D, Koeberle A, Werz O, Jauch J.* Total synthesis of myrtucommulone A. Angew Chem Int Ed 2010; 49: 2045–2049

15 *Gerbeth K, Meins J, Werz O, Schubert-Zsilavecz M, Abdel-Tawab M.* Determination of Myrtucommulone from *Myrtus communis* in human and rat plasma by liquid chromatography/tandem mass spectrometry. Planta Med 2011; 77: 450–454

16 *Shah V, Midha KK, Findley JWA, Hill HM, Hulse JD, McGilveray IJ, Mc Kay G, Miller KJ, Patnaik RN, Powell ML, Tonelli A, Viswanathan CT, Yacobi A.* Bioanalytical method validation – a revisit with a decade of progress. J Pharm Res 2000; 17: 1551–1557

17 *Edginton AN, Schmitt W, Willmann S.* Application of physiology-based pharmacokinetic and pharmacodynamic modeling to individualized target-controlled propofol infusions. Adv Ther 2006; 23: 143–158

18 *Willmann S, Hoehn K, Edginton A, Sevestre M, Solodenko J, Weiss W, Lippert J, Schmitt W.* Development of a physiology-based whole-body population model for assessing the influence of individual variability on the pharmacokinetics of drugs. J Pharmacokinet Pharmacodynam 2007; 34: 401–431

19 *Potthast H, Dressman JB, Junginger HE, Midha KK, Oeser H, Shah VP, Vogelpoel H, Barends DM.* Biowaiver monographs for immediate release solid oral dosage forms: Ibuprofen. J Pharm Sci 2005; 94: 2121–2131

20 *Yee S. In vitro* permeability across Caco-2 cells (colonic) can predict *in vivo* (small intestine) absorption in man-fact or myth. Pharm Res 1997; 14: 763–766

21 *Arthursson P, Karsson J.* Correlation between oral drug absorption in humans and apparent drug permeability coefficients in human intestinal epithelial (Caco-2) cells. Biochem Biophys Res Commun 1991; 175: 880–885

22 *Jachak SM.* PGE synthase inhibitors as an alternative to COX-2 inhibitors. Curr Opin Investig Drugs 2007; 8: 411–415